Electronic tuning of β-diketiminate ligands with fluorinated substituents: effects on the O_2-reactivity of mononuclear Cu(I) complexes†‡

Lyndal M. R. Hill, Benjamin F. Gherman, Nermeen W. Aboelella, Christopher J. Cramer and William B. Tolman*

Received 12th July 2006, Accepted 14th August 2006
First published as an Advance Article on the web 31st August 2006
DOI: 10.1039/b609939d

Copper(I) complexes with the β-diketiminate ligands HC{C(R)N(Dipp)}{C(R′)N(Dipp)}$^-$ (Dipp = $C_6H_3{}^iPr_2$-2,6; L^1, R = CF_3, R′ = CH_3; L^2, R = R′ = CF_3) have been isolated and fully characterized. On the basis of X-ray structural comparisons with the previously reported complex LCu(CH_3CN) (L = HC{C(CH_3)N(Dipp)}$_2^-$), the ligand environments at the copper centers in the analogous nitrile adducts with L^1 and L^2 impose similar steric demands. L^1Cu(CH_3CN) reacts instantaneously at low temperature with O_2 to form a thermally-unstable intermediate with an isotope-sensitive vibration at 977 cm^{-1} (928 cm^{-1} with $^{18}O_2$), in accord with the peroxo O–O stretch associated with side-on coordination for LCu(O_2). However, L^2Cu(CH_3CN) is unreactive toward O_2 even at room temperature. Evaluation of the redox potentials of the nitrile adducts and the CO stretching frequencies of the carbon monoxide adducts revealed an incremental adjustment of the electronic environment at the copper center that correlated with the extent of ligand fluorination. Furthermore, theoretical calculations (DFT, CASPT2) predicted that an increasing extent of Cu(II)–superoxo character and end-on coordination of the O_2 moiety in the Cu/O_2 product (L^2 > L^1 > L) are accompanied by increases in the free energy for the oxygenation reaction, with L^2 unable to support a Cu/O_2 intermediate. Calculations also predict the 1 : 1 Cu/O_2 adducts to be unreactive with respect to hydrogen atom abstraction from hydrocarbon substrates on the basis of their stability towards both reduction and protonation.

Introduction

A key step in many oxidation reactions of biological and industrial importance is the binding and activation of dioxygen at a single copper center to yield 1 : 1 Cu/O_2 species.[1,2] Understanding how ligand structural effects control the geometries, electronic structures, and reactivity of such species is a primary objective of current research aimed ultimately at obtaining mechanistic insight into oxidation catalysis.[1,3] Structurally characterized examples of 1 : 1 Cu/O_2 species are limited to a trapped form of peptidylglycine α-hydroxylating monooxygenase (PHM)[4] and the synthetic complexes **1**–**4** (Fig. 1).[5–8] X-ray crystallographic, spectroscopic, and theoretical data support Cu(II)–superoxide formulations for **1** and **2**,[5,6] whereas **3** and **4** have significant Cu(III)-peroxo character.[7–10] The latter electronic structure derives from the nature of the β-diketiminate and anilido-imine supporting ligands, which through powerful electron donation stabilize the high oxidation state of the metal ion and drive the reduction of the dioxygen moiety to the peroxide level. Unfortunately, these effects also appear to render **3** and **4** relatively unreactive,[11] limiting efforts to test the hypothesized involvement of 1 : 1 Cu/O_2 species in organic substrate hydroxylations (*e.g.* in PHM).[12] We therefore asked: How will decreasing the electron donation of the β-diketiminate ligand influence the Cu(I)/O_2 reactivity?

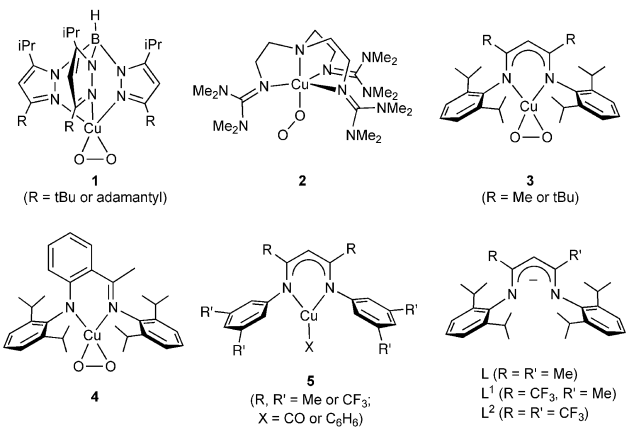

Fig. 1 Structurally defined 1 : 1 Cu/O_2 adducts and the ligand used in this study (L, L^1, and L^2)

Previous studies have shown that electronic influences of ligand substituent variation on Cu(I)/O_2 reactions can be significant. Karlin and coworkers reported that electron-donating 4-methoxy or -amino substituents on the pyridyl donors of poly(pyridyl)alkylamine ligands significantly influence the oxygenation kinetics of Cu(I) complexes, the ratio and spectroscopic

Department of Chemistry, Center for Metals in Biocatalysis, and Supercomputer Institute, University of Minnesota, 207 Pleasant St. SE, Minneapolis, MN 55455-0431, USA. E-mail: tolman@chem.umn.edu; Fax: +1 612-624-7029; Tel: +1 612-625-4061

† The HTML version of this article has been enhanced with additional colour images.

‡ Electronic supplementary information (ESI) available: NMR spectra, X-ray structures of LCuCO, L^2CuCO, and L^2Cu(CH_3CN), cyclic voltammograms, UV-vis spectra, and selected results of theoretical calculations, and atomic coordinates for all computed structures. See DOI: 10.1039/b609939d

properties of the resulting μ-η^2:η^2-peroxo and bis(μ-oxo)dicopper products, and their reactivity with added substrates.[13,14] Some of these effects have been examined by theory,[15] and related results were reported by Itoh and coworkers upon variation of the alkylamine groups in similar ligands.[16] Extensive data on the electronic effects of CF_3 substituents in tris(pyrazolyl)hydroborate (Tp) complexes of Cu(I) have been published, with the ν(CO) values for TpCu(I)–CO compounds being particularly useful indicators of the electron density at the metal.[17] Gorun and coworkers observed stabilization of a peroxodicopper complex by a CF_3-substituted Tp ligand, which appears to derive from a combination of steric and electronic factors.[18,19] Perhaps most germane to our work is the study by Sadighi and coworkers of Cu(I) complexes **5** (X = C_6H_6), in which incorporation of the CF_3 groups resulted in observation of arene substituent hydroxylation upon room temperature oxygenation.[20] Copper(I) complexes of related fluorinated triazapentadienide ligands also have been characterized, but no O_2 reactivity was reported.[21]

Herein, we report a systematic study aimed at assessing electronic effects at parity of steric factors on the properties of Cu(I) complexes of L (R = R′ = Me, Fig. 1) and derivatives in which the backbone methyl substituents are replaced by one (L^1) or two (L^2) CF_3 groups. The course of their low temperature oxygenations are presented, along with theoretical calculations which provide electronic and structural insights into the observed chemistry.

Experimental

General considerations

All reagents were obtained from commercial sources and used without further purification, unless otherwise stated. Reagent grade 2,6-diisopropylaniline (90%) was freshly distilled from CaH_2. Deuterated benzene and THF were dried over Na/benzophenone and vacuum transferred. Toluene, THF, pentane and Et_2O were passed through solvent purification columns (Glass Contour, Laguna, CA). Acetonitrile was passed through a solvent purification column (M-Braun) and further dried over activated 3 Å molecular sieves. Acetone (protio and deuterated forms) was vacuum transferred from $CaSO_4$ before drying over activated 3 Å molecular sieves (2–3 cycles). All metal complexes were prepared and stored in a Vacuum Atmospheres inert atmosphere glove-box under a dry nitrogen atmosphere or were manipulated using standard inert atmosphere vacuum and Schlenk techniques. The reagents $(Me_3SiCH_2Cu)_4$,[22] HL^2,[23] and $LCu(CH_3CN)$[24] were prepared according to literature procedures. Labeled dioxygen ($^{18}O_2$, and 50% statistical ^{18}O mixed-label gas) was purchased from Icon Isotopes, Inc.

Physical methods

NMR spectra were recorded on a Varian VI-500 or VI-300 spectrometer. NMR spectra were referenced internally to the solvent (for benzene: 128.39 ppm for ^{13}C NMR and 7.16 ppm in ^1H NMR for residual protio solvent). UV-Vis spectra were recorded on an HP8453 (190–1100 nm) diode array spectrophotometer. Low-temperature spectra were acquired using a Unisoku cryostat-controlled UV-Vis cell holder. Solutions of Cu(I) complexes were placed in anaerobic cuvettes sealed with rubber septa. Oygenations were carried out by bubbling dry O_2 gas through the analyte solution at ambient pressure. Excess O_2 was removed by purging the resulting solution with dry Ar gas. Samples for resonance Raman spectroscopy were formed by creating a headspace of $^{16}O_2$ over a solution of the Cu(I) complex in a Schlenk flask at −80 °C or by adding ~10 mL of $^{18}O_2$ or $^{16}O^{18}O$ (50% ^{18}O) to a frozen solution of the Cu(I) complex (−196 °C) and reacting the mixture at −80 °C. Solutions were prepared in acetone with Cu(I) complex concentrations of 12.5 mM for the $^{16}O_2$ and $^{18}O_2$ reactions, and 18.0 mM for the $^{16}O^{18}O$ reaction. Resonance Raman spectra were collected on an Acton AM-506 spectrometer using a Princeton Instruments liquid N_2 cooled (LN1100-PB) CCD detector and ST-1385 controller interfaced with Winspec software. A Spectra-Physics BeamLok 2060-KR-V Krypton ion laser was used to excite at 413.1 nm. The spectra were obtained at −196 °C using a backscattering geometry; samples were frozen in a copper cup attached to a liquid nitrogen cooled coldfinger. The spectral window was calibrated with liquid indene and spectra were internally referenced to solvent. Baseline corrections (polynomial fits) were carried out using Grams32/Spectral Notebase Version 4.04 (Galactic). Cyclic voltammograms were recorded using Pt working and auxiliary electrodes, a Ag wire/$AgNO_3$ (10 mM in CH_3CN) reference electrode, and a BAS Epsilon potentiostat connected to a 22 mL cell in an inert-atmosphere glovebox. Experiments were performed on analyte solutions of 1 mM in THF with 0.3 M Bu_4NPF_6 (sample volumes of ~5 mL) at room temperature. The ferrocene/ferrocenium couple was recorded for reference, using the reported value of $E_{1/2}$ = + 560 mV *vs.* SCE (for 0.1 M Bu_4NPF_6 in THF).[25] FT-IR spectra were recorded using a CaF_2 solution cell (International Crystal Labs) in an Avatar 370 spectrometer (ThermoNicolet). Elemental analyses were performed by Robertson Microlit (Madison, NJ). ESI-MS were recorded on a Bruker BioTOF II instrument.

X-Ray crystallography

Crystals of an appropriate size were placed onto the tip of a 0.1 mm diameter glass capillary and mounted on either a Siemens or Bruker SMART Platform CCD diffractometer.[26] Data collections were carried out using Mo Kα radiation at 173 K, with a detector distance of ~4.9 cm. A randomly oriented region of reciprocal space was surveyed to the extent of one sphere and to a resolution of 0.77 Å (L^1 or $L^2Cu(CH_3CN)$), 0.80 Å ($L^2Cu(CO)$), and 0.84 Å (LCu(CO)). Four major sections of frames were collected with 0.30° steps in ω at four different ϕ settings and a detector position of −28° in 2θ. The intensity data were corrected for absorption and decay (SADABS).[27] Final cell constants were calculated from the *xyz* centroids of strong reflections from the actual data collection after integration (SAINT).[28] See ESI‡ for full crystal and refinement details in the form of CIFs.

CCDC reference numbers 614585–617544.

For crystallographic data in CIF or other electronic format see DOI: 10.1039/b609939d

HL^1

In a 500 mL Schlenk flask, 2,6-diisopropylaniline (32 mL, 152.5 mmol) was combined with toluene (60 mL). The solution was cooled in an ice–ethanol bath (≤ −10 °C) under a stream of

argon. A solution of $TiCl_4$ (6.0 mL, 54.6 mmol) in toluene (10 mL) was added by cannula over 15 min. The reaction mixture turned brown and contained much insoluble material with about half of the $TiCl_4$/toluene mixture added. The reaction was gradually warmed from −10 °C to 26 °C and stirred for 1 d. 1,1,1-Trifluoro-2,4-pentanedione (3.0 mL, 24.8 mmol) was added dropwise to the stirred mixture. With about a third of the dione added the reaction turned yellow–orange and required addition of further toluene (60 mL) to assist stirring. The reaction flask was fitted with a reflux condenser and submerged in an oil bath. The mixture was heated at 88 °C (oil bath temperature) for 3 d, then at reflux for a further 2 d. The cooled yellow sludgy-mixture was filtered under vacuum and the red–brown filtrate washed with distilled water (3 × 100 mL). Solvents were removed on a Schlenk line using a water bath at 50 °C. The red residue was purified by column chromatography on silica gel using dichloromethane ($R_f = 0.92$). Recrystallisation from hot methanol or ethanol afforded crystalline, yellow material. Yield: 1.39 g (12%). ^{1}H NMR (500 MHz, benzene-d_6): δ 1.07 (d, 6H, $^3J_{HH} = 6.5$ Hz), 1.12 (apparent t—two overlapping doublets, 12H, $^3J_{HH} = 7.3$ Hz) and 1.31 (d, 6H, $^3J_{HH} = 7.5$ Hz): (CH_3)$_2$CH, 1.51 (s, 3H, CH_3 of ligand backbone), 3.11 (sept, 2H, $^3J_{HH}$ = 6.8 Hz) and 3.29 (sept, 2H, $^3J_{HH} = 6.8$ Hz), CH(CH$_3$)$_2$, 5.40 (s, 1H, CH of ligand backbone), 7.07–7.18 (m, integration obscured by protio-solvent peak, aromatic CH of phenyl rings), 12.12 (s, 1H, NH) ppm. ^{13}C NMR (75 MHz, relax. delay = 8 s, benzene-d_6), δ 21.12 (CH$_3$ of ligand backbone), 23.30, 23.83, 24.79 and 25.52: (CH_3)$_2$CH, 28.96 and 29.24 (*C*H(CH$_3$)$_2$), 90.58 (q, $^3J_{CF}$ = 3.8 Hz, *C*H of ligand backbone), 120.83 (q, $^1J_{CF} = 284.5$ Hz, *C*F$_3$), 123.78, 124.24, 126.23 and 127.56 (*C*H of phenyl rings), 138.74, 141.04, 141.75 and 143.60 (quaternary C of phenyl rings), 150.23 (q, $^2J_{CF}$ = 26.9 Hz, quaternary C of ligand backbone, *C*CF$_3$), 164.02 (quaternary C of ligand backbone, *C*CH$_3$) ppm. ESI-MS (low resolution): m/z 473.3 [M + H$^+$]. Anal. Calc. for $C_{29}H_{39}F_3N_2$: C, 73.70; H, 8.32; N, 5.93. Found: C, 73.61; H, 8.60; N, 6.15.

(L^1 or L^2)Cu(CH$_3$CN). General procedure

The ligand precursor HL^1 or HL^2 (200 mg) was dissolved in CH$_3$CN (10 mL) and added dropwise to (Me$_3$SiCH$_2$Cu)$_4$ (1 mol. eq. Cu) with stirring in a reaction vessel protected from light. The reaction mixture was vigorously stirred for 1–2 d, the solvent removed and the residue dissolved in CH$_3$CN (~2 mL). The solution was filtered through a 0.2 micron filter disk before refrigeration at −20 °C. Large crystals formed, and these were separated from the mother liquor and washed with cold pentane. The washings and mother liquor were combined, the solvent removed and the residue dissolved in CH$_3$CN in order to produce further crop(s) of crystals upon refrigeration at −20 °C.

L^{1}Cu(CH$_3$CN). . Yield: 97%. ^{1}H NMR (500 MHz, benzene-d_6): δ 0.00 (s, 3H, CH_3CN), 1.23 (d, 6H, $^3J_{HH} = 7.0$ Hz), 1.36 (d, 6H, $^3J_{HH}$ = 7.0 Hz) and 1.40 (apparent t—two overlapping doublets, 12H, $^3J_{HH}$ = 6.3 Hz): (CH_3)$_2$CH, 1.71 (s, 3H, CH_3 of ligand backbone), 3.35 (sept, 2H, $^3J_{HH}$ = 6.8 Hz) and 3.56 (sept, 2H, $^3J_{HH} = 6.8$ Hz): (CH$_3$)$_2$CH, 5.56 (s, 1H, CH of ligand backbone), 7.03–7.15 (m, 6H, Ar–CH of phenyl rings) ppm. ^{13}C NMR (125 MHz, benzene-d_6): δ 0.23 (*C*H$_3$CN), 23.19, 23.55, 23.84, 24.82 and 25.54 (all (CH_3)$_2$CH, and *C*H$_3$ of ligand backbone), 28.57 and 28.90 ((CH$_3$)$_2$*C*H), 89.16 (q, $^3J_{CF}$ = 4.5 Hz, *C*H of ligand backbone), 116.88 (CH$_3$*C*N), 122.57 (q, $^1J_{CF}$ = 286.4 Hz, *C*F$_3$), 123.26, 123.85, 124.10 and 124.73 (*C*H of phenyl rings), 140.01, 141.27, 147.39 and 148.14 (quaternary C of phenyl rings), 149.04 (q, $^2J_{CF}$ = 23.9 Hz, quaternary C of ligand backbone, *C*CF$_3$), 166.43 (quaternary C of ligand backbone, *C*CH$_3$) ppm. Anal. Calc. for $C_{31}H_{41}CuF_3N_3$: C, 64.62; H, 7.17; N, 7.29. Found: C, 64.45; H, 7.40; N, 7.32.

L^{2}Cu(CH$_3$CN). Yield: 76%. ^{1}H NMR (500 MHz, benzene-d_6): δ − 0.02 (s, 3H, CH_3CN), 1.34 (apparent t—two overlapping doublets, 24H, $^3J_{HH} = 6.5$ Hz, (CH_3)$_2$CH), 3.35 (sept, 4H, $^3J_{HH}$ = 6.8 Hz, CH(CH$_3$)$_2$), 6.19 (s, 1H, CH of ligand backbone), 7.00–7.10 (m, 6H, Ar–CH of phenyl rings) ppm. ^{13}C NMR (75 MHz, benzene-d_6): δ 0.03 (*C*H$_3$CN), 22.95 and 25.49 ((*C*H$_3$)$_2$CH), 28.98 (*C*H(CH$_3$)$_2$), 83.94 (sept, $^3J_{CF}$ = 5.1 Hz, *C*H of ligand backbone), 121.68 (q, $^1J_{CF}$ = 286.1 Hz, *C*F$_3$), 117.24 (CH$_3$*C*N), 123.43 and 125.08 (*C*H of phenyl rings), 140.33 and 146.19 (quaternary C of phenyl rings), 151.67 (q, $^2J_{CF}$ = 24.8 Hz, quaternary C of ligand backbone) ppm. Anal. Calc. for $C_{31}H_{38}CuF_6N_3$: C, 59.08; H, 6.08; N, 6.67. Found: C, 58.99; H, 5.85; N, 6.66.

(L, L^1, or L^2)Cu(CO). General procedure

The complex (L, L^1, or L^2)Cu(CH$_3$CN) (29 μmol) was dissolved in THF (2 mL) in a 10 mL Schlenk tube and stirred under a CO headspace at ambient pressure for 2 h, during which the solvents were evaporated. Half of the dried solid (pale yellow to yellow) was dissolved in THF (0.4 mL) and the IR-spectrum recorded immediately (CaF_2); NMR analysis indicated quantitative conversion to the carbonyl adducts. After several days at −20 °C, pentane solutions of (L or L^2)Cu(CO) produced yellow crystals which were appropriate for X-ray structural analyses. Elemental analyses were also performed on samples of these crystals.

LCu(CO). ^{1}H NMR (500 MHz, benzene-d_6): δ 1.20 (d, 12H, $^3J_{HH} = 7.0$ Hz) and 1.29 (d, 12H, $^3J_{HH} = 7.0$ Hz): (CH_3)$_2$CH; 1.73 (s, 6H, CH_3 of ligand backbone), 3.35 (sept, 4H, $^3J_{HH}$ = 6.8 Hz, CH(CH$_3$)$_2$), 4.98 (s, 1H, CH of ligand backbone), 7.09–7.15 (m, 6H, CH of phenyl rings) ppm. ^{13}C NMR (125 MHz, benzene-d_6): δ 23.31, 23.62, 24.88, 28.52, 95.49, 124.05, 125.44, 140.73, 149.35, 164.97, 178.42 ppm. FT-IR (THF): 2070 cm^{-1} (ν_{CO}). Anal. Calc. for $C_{30}H_{41}CuN_2O$: C, 70.76; H, 8.12; N, 5.50. Found: C, 70.96; H, 8.02; N, 5.39.

L^{1}Cu(CO). ^{1}H NMR (500 MHz, benzene-d_6): δ 1.12 (d, 6H, $^3J_{HH} = 7.0$ Hz), 1.21 (d, 6H, $^3J_{HH} = 7.0$ Hz), 1.26 (d, 6H, $^3J_{HH}$ = 7.0 Hz) and 1.31 (d, 6H, $^3J_{HH} = 7.0$ Hz): (CH_3)$_2$CH; 1.57 (s, 3H, CH_3 of ligand backbone), 3.09 (sept, 2H, $^3J_{HH} = 6.8$ Hz) and 3.34 (sept, 2H, $^3J_{HH} = 6.8$ Hz): CH(CH$_3$)$_2$; 5.55 (s, 1H, CH of ligand backbone), 7.07–7.13 (m, 6H, CH of phenyl rings) ppm. ^{13}C NMR (125 MHz, benzene-d_6): δ 22.94, 23.38, 23.53, 24.72, 25.66, 28.59, 28.88, 91.00 (q, $^3J_{CF} = 4.9$ Hz), 122.05 (q, $^1J_{CF} = 285.1$ Hz), 123.68, 124.27, 125.86, 126.15, 139.77, 141.27, 147.50, 148.07, 150.32 (q, $^2J_{CF}$ = 24.3 Hz), 168.65, 176.39 ppm. FT-IR (THF): 2083 cm^{-1} (ν_{CO}).

L^{2}Cu(CO). ^{1}H NMR (500 MHz, benzene-d_6): δ 1.17 (d, 12H, $^3J_{HH} = 7.0$ Hz) and 1.24 (d, 12H, $^3J_{HH} = 7.0$ Hz): (CH_3)$_2$CH; 3.09 (sept, 4H, $^3J_{HH} = 6.8$ Hz, CH(CH$_3$)$_2$), 6.18 (s, 1H, CH of ligand backbone), 7.05 (br s, 6H, CH of phenyl rings) ppm. ^{13}C NMR (125 MHz, benzene-d_6): δ 22.84, 25.55, 28.95, 85.73 (sept,

$^3J_{CF} = 5.1$ Hz), 121.14 (q, $^1J_{CF} = 285.5$ Hz), 123.89, 126.62, 140.18, 146.37, 153.52 (q, $^2J_{CF} = 25.6$ Hz), 174.53 ppm. FT-IR (THF): 2097 cm^{-1} (ν_{CO}). Anal. Calc. for $C_{30}H_{35}CuF_6N_2O$: C, 58.38; H, 5.72; N, 4.54. Found: C, 58.32; H, 5.57; N, 4.39.

$L^1Cu(O_2)$

UV-Vis: A Beer–Lambert plot was constructed for replicate oxygenations of $L^1Cu(CH_3CN)$ in THF at −80 °C (0.2–0.6 mM); [λ_{max}, nm (ε, M^{-1} cm^{-1})]: 415 (sh, 1780), 540 (125). Resonance Raman ($\lambda_{ex} = 413.1$ nm, 77 K, acetone): 977 ($^{16}O_2$), 955 ($^{16}O^{18}O$), 928 ($^{18}O_2$) cm^{-1}.

Computational Methods: A. Density functional calculations

Geometry optimizations were carried out using the Jaguar suite, version 6.1, of *ab initio* quantum chemistry programs.[29] Density Functional Theory (DFT) with the B3LYP functional[30–32] was used in all calculations, as this functional has proven successful in predicting ligand–Cu(I) and –Cu(II) bond dissociation energies.[33] Computations on singlet and triplet states employed restricted (RDFT) and unrestricted (UDFT) levels of theory, respectively, in keeping with the established methodology for dealing with complexes between Cu(I) and dioxygen.[7b,8,11b,34,35] For copper, the lacvp** effective core potential basis set[36] was used, while 6-31G** was used for all other atoms.

Relative electronic differences between various oxygenated species were measured using Mulliken charge populations. Such analyses, when founded on DFT calculations carried out with balanced basis sets, have been effective at tracking electron flow in a variety of reactions involving the reaction of dioxygen at a metal center.[7b,8,37,38]

Analytical vibrational frequency calculations were carried out to verify optimized geometries as stationary points and to allow for zero-point energy, enthalpy, and entropy corrections to be made (and, hence, free energies to be computed). In order to make these calculations more tractable, truncated models were employed for L, L^1, and L^2 (Fig. 1), in which the four isopropyl groups on the flanking 2,6-diisopropylphenyl rings were changed to hydrogen atoms. The positions of these hydrogen atoms were optimized with the remainder of the structure held fixed prior to the frequency calculations. In subsequent calculations, the full models were reoptimized with B3LYP, using the 6-311G** triple-ζ plus polarization basis set for all atoms, except Cu, on which the LACV3P** basis set (a triple-ζ basis compatible with the effective core potential)[36] was used. The O–O stretch frequencies determined from vibrational frequency calculations on truncated models derived from these triple-ζ geometries were used for comparison with those determined spectroscopically,[9] following scaling by a factor of 0.97.[39]

Single-point solvation energies were calculated for each optimized geometry using the self-consistent reaction field method as implemented in the Poisson–Boltzmann solver in Jaguar.[40,41] The solvent was taken to be THF, in order to facilitate comparison with experimental results, with dielectric constant ε equal to 7.43 at 25 °C and 12.27 at −80 °C.[42,43]

A Born–Haber free energy cycle (Scheme 1a) was used to determine pK_b values. The free energy change for deprotonation in aqueous solution was determined according to eqn (1),

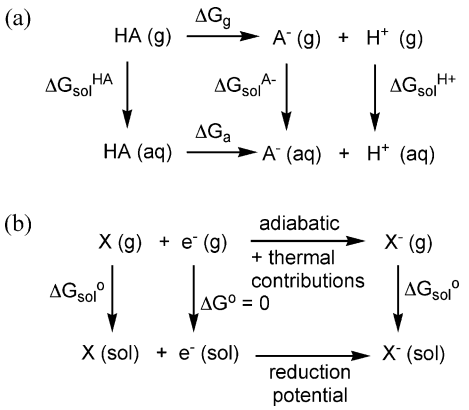

Scheme 1 Free energy cycles used to determine (a) pK_b values and (b) reduction potentials (see text).

$$\Delta G_a = \Delta G_g - \Delta G_{sol}^{HA} + \Delta G_{sol}^{A-} + \Delta G_{sol}^{H+} \quad (1)$$

where ΔG_g is the gas-phase deprotonation energy and ΔG_{sol}^{HS}, ΔG_{sol}^{A-}, and ΔG_{sol}^{H+} are the solvation free energies for the conjugate acid and base forms and the proton, respectively. The solvation free energy for the proton is taken to be −265.9 kcal mol^{-1} prior to correcting for the 1 atm to 1 M standard-state change.[44] The pK_b is given by eqn (2), where R is the universal gas constant and T is temperature.

$$pK_b = 14.0 - \frac{\Delta G_a}{2.303RT} \quad (2)$$

A free energy cycle was also used to calculate adiabatic reduction potentials (Scheme 1b). ΔG_r, the free energy change for reduction in solution, is given by

$$\Delta G_r = G_g^{X-} - G_g^{X} + \Delta G_{sol}^{X-} - \Delta G_{sol}^{X} \quad (3)$$

where G_g^{X-} and G_g^{X} are gas phase free energies for the reduced and oxidized species and ΔG_{sol}^{X-} and ΔG_{sol}^{X} are their respective solvation energies. The absolute reduction potential is computed by eqn (4),

$$E^\circ = -\frac{\Delta G_r}{nF} \quad (4)$$

where F is the Faraday constant and n is the number of electrons transferred. Subtracting 4.28 V[45] from E° in eqn (4) yields the potential relative to the standard hydrogen electrode (SHE). Systematic error in the computation of the reduction potentials was accounted for using an empirical correction. Having a copper coordination environment similar to that with the β-diketiminate ligand and having been well characterized with respect to its electrochemistry, a copper complex supported by a triazamacrocyclic ligand was chosen as the reference system.[46] Its measured Cu(III)/Cu(II) reduction potential was −0.271 V *vs.* SHE, whereas the computed reduction potential was 0.485 V, implying the correction factor to be −0.76 V. The viability of transferring such corrections between closely related systems has been established.[47]

B. Multireference calculations

Closed-shell singlet and high-spin triplet Kohn–Sham wave functions can be expressed as single Slater determinants. However, a minimum of two determinants is required to describe open-shell singlets, which therefore cannot be rigorously expressed within the framework of Kohn–Sham DFT. This shortcoming

of DFT is particularly relevant to calculations on complexes between Cu(I) and dioxygen.[48] These species typically possess nontrivial degrees of Cu(II)–superoxo character, which may be considered to be biradical, with one electron localized to Cu(II) and the other to superoxide. In order to rigorously account for the multideterminantal nature of the singlet 1 : 1 Cu/O_2 adducts, single-point multireference second-order perturbation theory (CASPT2) was used.[49]

In order to render the inherently expensive CASPT2 calculations computationally feasible, procedure dictates changing both the backbone CH_3/CF_3 groups and flanking 2,6-diisopropylphenyl groups of the β-diketiminate ligand to hydrogen atoms prior to the CASPT2 calculations.[7,8,11,35] Singlet–triplet energy splittings are computed at the DFT and CASPT2 levels for these small models, enabling the quantity Δ to be computed (eqn (5)). With triplet states being well described by DFT, the relative energy difference between the DFT and CASPT2 values for the triplet energy can be taken as zero. Δ then becomes a measure of the relative energy difference of the singlet states between the two levels of theory and can be used as a correction to the DFT energies for the singlet states. Final energies for the full model system are obtained by combining the DFT energy for the full model with the Δ value for the corresponding small model system. In previous work examining the oxygenation of $LCu(CH_3CN)$ (Fig. 1),[7] we established that Δ linearly correlates with the Cu–O bond length in the case of both side-on and end-on dioxygen coordination to copper, and this result is used to expedite the determination of Δ for the neutral singlet Cu/O_2 adducts examined here. For the protonated forms of the 1 : 1 adducts, single-point multireference second-order perturbation theory (CASPT2) was used.[50] The initial complete active space (CAS) of the reference wave function was comprised of 18 electrons in 12 orbitals originating from the Cu valence orbitals and electrons and the dioxygen σ_{2p}, σ_{2p}*, π_{2p}, and π_{2p}* orbitals and electrons. Eliminating doubly occupied orbitals led to a final (12,9) active space. A 17-electron relativistic effective core potential basis was used for Cu[51] in these calculations, with a polarized double-ζ atomic natural orbital basis[48] being employed for all other atoms.

$$\Delta = ({}^1A - {}^3A)_{CASPT2} - ({}^1A - {}^3A)_{DFT} = [({}^1A)_{CASPT2} - ({}^1A)_{DFT}] - [({}^3A)_{CASPT2} - ({}^3A)_{DFT}] \quad (5)$$

This procedure involving a combination of DFT and CASPT2 calculations has proven to reliably account for the multideterminantal nature of singlet 1 : 1 Cu/O_2 adducts which occur in biomimetic[7] and active site modeling[52] of DβM and PHM. The methodology has yielded singlet–triplet state orderings consistent with spectroscopic data for the adducts.[7b,8,53] Experimental kinetics data for the oxygenation of LCu(MeCN) was also well reproduced using this computational methodology.[7b]

Results

Synthesis and structural characterization of copper(I) complexes

The complex $LCu(CH_3CN)$ was prepared from LiL and $[Cu(CH_3CN)_4](CF_3SO_3)$, as previously reported.[24] HL^1 was synthesized in a similar manner to HL^2 by a one-pot reaction, with the first step being the activation of 2,6-diisopropylaniline by coordination to titanium.[23] The overall reaction (Scheme 2) utilizes

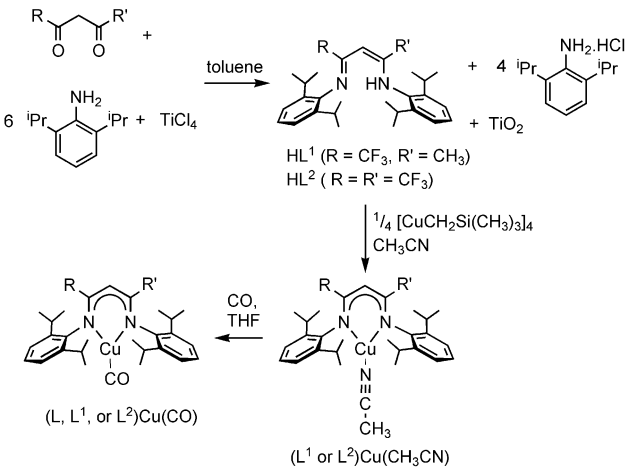

Scheme 2 Synthesis of ligands and complexes.

2,6-diisopropylaniline both in the double condensation and in the removal of HCl from the reaction mixture, with the concomitant formation of TiO_2 providing the driving force. Upon addition of the asymmetric ketone 1,1,1-trifluoro-2,4-pentanedione to the $TiCl_4$/diisopropylaniline mixture, prolonged reflux was required before HL^1 was detected by ESI-MS. Isolation of HL^1 necessitated the use of column chromatography and recrystallisation. Initial unsuccessful efforts toward the synthesis of HL^1 included a similar reaction progression for the condensation, employing $AlMe_3$ to activate the 2,6-diisopropylaniline N-donor. The failure of this approach is unsurprising given the low-yielding $TiCl_4$-assisted condensation.

The complexes (L^1 or L^2)$Cu(CH_3CN)$ were cleanly prepared in high yields (97 and 76%, respectively) by direct reaction of the corresponding ligands with the copper–alkyl reagent $[CuCH_2Si(CH_3)_3]_4$ in acetonitrile (Scheme 2). In both cases, crystals obtained from the reaction mixture were analytically pure and suitable for X-ray structural determinations. Furthermore, solids obtained by solvent evaporation from the reaction mixture were free of contaminants (NMR), making this method convenient for preparing Cu(I) complexes of high purity. The ^1H and ^{13}C NMR spectra were fully assigned on the basis of splitting patterns, coupling constants (*e.g.*, J_{CF}) and 2D correlations from HMQC and HMBC experiments (Fig. S1, for example).‡ The complexes (L, L^1 or L^2)Cu(CO) were formed by taking a THF solution of the parent Cu(I)–acetonitrile complex to dryness under a carbon monoxide atmosphere. The solids were characterized by ^1H and ^{13}C NMR and FT-IR, which indicated complete loss of acetonitrile, with the only impurity being trace THF. Crystals of (L or L^2)Cu(CO) were further characterized, with elemental analyses and X-ray structures (Fig. S2 and S3, respectively)‡ confirming the presence of the terminal CO ligand. This series augments the previously reported complexes **5** (X = CO), the only other examples of Cu(I)–CO complexes supported by β-diketiminate ligands.[20]

X-Ray structural determinations were performed for $L^1Cu(CH_3CN)$ (Fig. 2) and $L^2Cu(CH_3CN)$ (Fig. S4). ‡The structures are very similar to that of $LCu(CH_3CN)$.[24] The Cu centers are trigonally coordinated by the three nitrogen donors, with the bite-angle of the β-diketiminate (BDI) ligand (~99°) somewhat smaller than the N_{BDI}–Cu–$N_{nitrile}$ angles (~129–132°)

Table 1 Selected bond distances (Å) and angles (°)[a]

Bond or Angle	LCu(CH_3CN)[b]	L^1Cu(CH_3CN)	L^2Cu(CH_3CN)
Cu–N1	1.9404(16)	1.9431(14)	1.9398(14)
Cu–N2	1.9425(17)	1.9307(16)	1.9352(14)
Cu–N3	1.864(2)	1.8656(16)	1.8698(16)
N1–Cu–N2	98.98(7)	99.04(6)	98.98(6)
N1–Cu–N3	131.75(8)	130.10(7)	128.93(7)
N2–Cu–N3	129.25(8)	130.78(7)	131.78(7)
C2–N1–C6	118.92(17)	122.91(15)	124.74(14)
C4–N2–C18	119.23(17)	119.34(16)	125.00(14)

[a] Estimated standard deviations are in parentheses. [b] The numbering scheme for this structure is in accord with the CCDC entry (XIGWIT), though differing slightly from the CIF accompanying ref. 24 (for which C6 and C18 appear as C11 and C31, respectively).

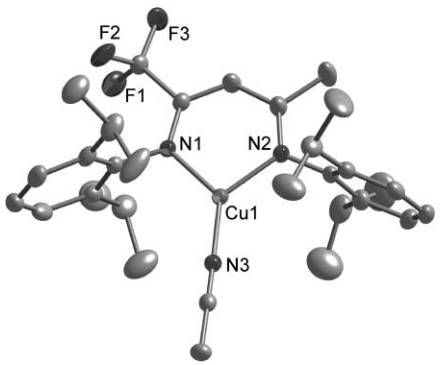

Fig. 2 Representation of the X-ray structure of L^1Cu(CH_3CN), showing all nonhydrogen atoms as 50% thermal ellipsoids. Unlabeled atoms are carbons.

(Table 1). The steric environments provided by L^1 and L^2 are essentially the same as that of L, as gauged by the non-perturbed C_α–N_{BDI}–C_{aryl} angles (~119–125°, Table 1, last two entries). The CF_3 substituent(s) are accommodated in the ligand backbone without a collapse of the aryl ring(s) toward the acetonitrile ligand. Thus, L, L^1 and L^2 represent a progression of ligands that differ in their electron donating capabilites (*vide infra*) while maintaining similar, demanding steric environments at the Cu(I) site.

DFT calculations were performed for the Cu(I) complexes, and good agreement between the optimized geometries and crystal structures was observed. Heavy-atom RMSD values between the two sets of structures are 0.028 Å, 0.040 Å, and 0.045 Å with L,[7] L^1, and L^2, respectively. In the calculated structures, Cu–$N_{nitrile}$ distances increase from 1.934 Å (L) to 1.970 Å (L^1) to 1.972 Å (L^2) as the electron-donating character of the β-diketiminate ligand is decreased by addition of the CF_3 groups. This trend is not possible to discern experimentally (Table 1) because the differences are the same order of magnitude as the estimated standard deviations in the interatomic distances. As with the Cu(I)–CH_3CN complex supported by the anilido-imine ligand in **4**,[8] no significant asymmetry occurs with respect to CH_3CN coordination in L^1Cu(CH_3CN), with a difference in the two N_{BDI}–Cu–$N_{nitrile}$ bond angles of only 0.68°.

Table 2 Properties of Cu(I) complexes of β-diketiminate ligands

Ligand	$E_{1/2}$/mV[a]	ν(CO)/cm^{-1}[b]
L	−96	2070
L^1	110	2083
L^2	411	2097

[a] Measured for Cu(I)–MeCN complex *vs.* Fc/Fc$^+$. Conditions: 25 °C, Bu_4NPF_6 in THF (0.3 M). [b] Measured for Cu(I)–CO complex (THF).

Effects of CF_3 groups on properties of Cu(I) complexes

We assessed the electronic influences of the CF_3 substituents by comparing (a) the redox potentials of the complexes (L, L^1 or L^2)Cu(CH_3CN) by cyclic voltammetry and (b) the ν(CO) values of the carbonyl complexes (L, L^1, or L^2)Cu(CO). Cyclic voltammograms of (L, L^1 or L^2)Cu(CH_3CN) measured in THF with Bu_4NPF_6 (0.3 M) as electrolyte exhibited reversible waves ($i_{pc}/i_{pa} \sim 1$, ΔE = 89–116 mV at 20 mV s^{-1}) that we attribute to the Cu(I/II) couple (Fig. S5).‡[54] The measured $E_{1/2}$ values are listed in Table 2. Substitution of one methyl group in L with a CF_3 moiety (L^1) results in a ~200 mV increase in the redox potential, consistent with electronic destabilization of the Cu(II) state by the electron withdrawing group.[55] Substitution with a second CF_3 group (L^2) results in a greater increase of ~300 mV. The $E_{1/2}$ value is sufficiently high (~+0.9 V *vs.* SCE) to suggest that reactivity of L^2Cu(CH_3CN) with O_2 would be thermodynamically unfavorable, to the extent that electron transfer impacts complex stability (see below).

The trend in ν(CO) values for (L, L^1, or L^2)Cu(CO) is also consistent with the expected effects of CF_3 substitution, with increases of ~13 cm^{-1} for exchange of each methyl group by a CF_3 unit. These increases reflect greater C–O bond order due to decreased electron back donation from the less electron rich Cu(I) center. Similar trends have been described for TpCu(I)CO complexes (Tp = tris(pyrazolyl)hydroborate), for which the effects of extensive substituent variations on ν(CO) values have been mapped.[17] While the β-diketiminate ligand is generally considered to be more electron donating than Tp,[56] it is noteworthy that the ν(CO) value for L^2Cu(CO) of 2097 cm^{-1} is essentially identical to that for the Cu(I)–CO complex of the Tp ligand having a CF_3 substituent at each pyrazolyl 3-position (2100 cm^{-1}). Finally, further support for the correlation of ν(CO) with the electron withdrawing effects of the CF_3 groups is provided by the trend in the carbonyl carbon chemical shifts in ^{13}C NMR spectra, which are 178.42, 176.39, and 174.53, respectively, for the complexes supported by L, L^1, and L^2.

O_2 Reactivity of Cu(I) complexes: A. Experiment

Solutions of (L^1 or L^2)Cu(CH_3CN) in THF were oxygenated at −80 °C, but only in the case of L^1Cu(CH_3CN) was an intermediate observed spectroscopically. No new features in the UV-vis spectrum were observed upon extensive oxygenation of L^2Cu(CH_3CN) between −80 and 25 °C. For L^1Cu(CH_3CN), UV-vis features at 415 (sh, ε = 1780 M^{-1}cm^{-1}) and 540 (ε = 125 M^{-1} cm^{-1}) nm appeared upon treatment with O_2, which decayed upon warming (Fig. S6).‡ The resonance Raman spectrum acquired using λ_{ex} = 413.1 nm (77 K, acetone) exhibited a peak at 977 cm^{-1} which

Table 3 Spectroscopic data for Selected Cu/O_2 Complexes

Complex	UV-vis (λ_{max} (ε))	ν(O–O) ($^{16}O_2/^{16}O^{18}O/^{18}O_2$)	Ref.
3 (R = Me)	385 (2400), 600 (200)	968/943/917	7
3 (R = tBu)	424 (2000), 638 (200)	961/937/912	7
4	390 (7600), 645 (250)	974/—/908	8
L^1CuO_2	415 (1780), 540 (125)	977/955/928	This work

shifted to 928 cm^{-1} when $^{18}O_2$ was used (Fig. 3). When a mixture of $^{18}O_2$, $^{16}O^{18}O$, and $^{16}O_2$ was used, the spectrum contained an additional band at 955 cm^{-1}. The UV-vis and resonance Raman data are similar to those reported for **3** and **4** (Table 3), and on this basis we assign the oxygenation product as an analogous side-on adduct L^1CuO_2. The ν(O–O) values for L^1CuO_2 are higher than those of **3** (R = Me or tBu) as would be expected for decreased reduction of the O_2 ligand in the system supported by the poorer electron donor L^1. However, the differences are small, indicating a relatively minor influence of the CF_3 substituent on the bonding in the CuO_2 unit.

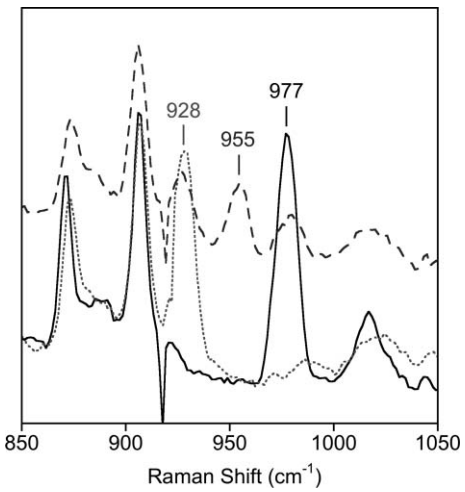

Fig. 3 Resonance Raman spectra of the product of oxygenation of $L^1Cu(CH_3CN)$ using $^{16}O_2$ (solid line), $^{18}O_2$ (dotted line), and a mixture of $^{16}O_2$, $^{16}O^{18}O$, and $^{18}O_2$ (dashed line). The peak positions of the O-isotope sensitive features are indicated.

B. Theory

For each ligand system and both end-on and side-on dioxygen coordination, singlet states are predicted by theory to be lower in energy than the corresponding triplet states by 2–10 kcal mol^{-1} (Table S1).‡ In the case of end-on dioxygen binding to copper, the singlet–triplet splitting remains fairly constant across the series of ligands. On the other hand, the triplet states become relatively more stable in the case of side-on O_2 coordination as Cu(II)–superoxide character increases with increasing ligand fluorination (*vide infra*). All subsequent discussion will focus on the singlet states of (L, L^1 or L^2)CuO_2 given their energetic stability over the triplet states.

The 4.7 kcal mol^{-1} preference for the η^2 versus η^1 dioxygen coordination in $LCuO_2$[7b] decreases by ~2 kcal mol^{-1} for each CF_3 group substituted onto the ligand backbone (Table 4). With L^2, end-on O_2 coordination to copper, as seen in the crystal structure for a precatalytic complex of PHM[4] and complex **2**,[6] is nearly isoenergetic with the side-on isomer. The free energy of oxygenation (−80 °C, THF) concurrently increments by ~5 kcal mol^{-1} with the addition of each CF_3 group (Table 4), such that oxygenation of the Cu(I)–CH_3CN complex, which was exergonic by 9.9 kcal mol^{-1} in the case of L, becomes slightly endergonic by 0.4 kcal mol^{-1} in the case of L^2. This marked increase is consistent with the inability to experimentally observe oxygenation of $L^2Cu(MeCN)$. With regards to synthesis of an end-on 1 : 1 Cu/O_2 adduct, a challenging reality is thus revealed here. Use of a less electron donating ligand (such as L^2) favors end-on dioxygen coordination, but copper complexes supported by such ligands are also markedly more difficult to oxygenate.

Table 4 Calculated free energy differences (η^2–η^1) between side-on (η^2) and end-on (η^1) singlet Cu/O_2 adducts supported by L, L^1, and L^2 and free energy changes (ΔG) for the oxygenation reaction[a]

Complex	η^2–η^1	ΔG
$LCuO_2$	−4.7[b]	−9.9[b]
L^1CuO_2	−2.4	−5.1
L^2CuO_2	−0.4	+0.4

[a] At −80 °C in THF, except as noted. All energies in kcal mol^{-1}. [b] −50 °C, THF (ref. 7*b*).

The O–O bond distances in the end-on adducts decrease by 0.006 Å with the addition of each CF_3 group from 1.281 Å in η^1-$LCuO_2$ to 1.269 Å in η^1-L^2CuO_2. Similarly, in the side-on cases, the O–O bond lengths shorten by 0.005 Å per CF_3 group leading from an O–O distance in η^2-$LCuO_2$ of 1.358 Å to 1.348 Å in η^2-L^2CuO_2. For $L^1Cu(CH_3CN)$, the asymmetry of the ligand backbone does not translate into asymmetric dioxygen binding. The N_{BDI}–Cu–$O_{proximal}$ angles in η^1-L^1CuO_2 differ by only 0.2°; the Cu–O distances in η^2-L^1CuO_2, by only 0.004 Å. Such virtually symmetric dioxygen coordination was also observed in the case with the asymmetric anilido-imine ligand, **4**.[8]

In addition to the trend in O–O bond distances between L, L^1, and L^2, computed O–O stretch frequencies increase by 8–9 cm^{-1} in both the end-on and side-on (L, L^1 or L^2)CuO_2 complexes for each CF_3 group substituted into the ligand backbone (Table 5). The magnitude of this change is close to that measured experimentally

Table 5 Computed ν(O–O) values for singlet end-on (η^1) and side-on (η^2) Cu/O_2 adducts[a]

Complex	η^1 ($^{16}O_2/^{16}O^{18}O/^{18}O_2$)	η^2 ($^{16}O_2/^{16}O^{18}O/^{18}O_2$)
$LCuO_2$	1238/1198/1165[b]	1042/1012/983[b]
L^1CuO_2	1247/1216/1175	1050/1022/991
L^2CuO_2	1256/1222/1185	1061/1032/1001

[a] Units: cm^{-1}. [b] Ref. 7*b*.

Table 6 Mulliken charge populations on the dioxygen fragment in singlet end-on (η^1) and side-on (η^2) Cu/O_2 adducts

Complex	η^1	η^2
$LCuO_2$	−0.43[a]	−0.60[a]
L^1CuO_2	−0.33	−0.52
L^2CuO_2	−0.32	−0.50

[a] Ref. 7*b*.

between L^1CuO_2 and **3** (R = Me; Table 3).[7] Comparison of the computed $\nu(^{16}O_2)$ and the differences $\Delta\nu(^{18}O_2) = \nu(^{16}O_2) - \nu(^{18}O_2)$ for η^1- and η^2-L^1CuO_2 supports the assignment of the experimental product obtained from oxygenation of $L^1Cu(CH_3CN)$ as the side-on 1 : 1 adduct (*cf.* Table 3).‡§ Experimentally non-resolvable ν(O–O) for the mixed label isotopomers ($Cu–^{16}O^{18}O$ *vs.* $Cu–^{18}O^{16}O$) were found in the end-on cases, providing more examples where mixed label resonance Raman experiments are not diagnostic for the mode of coordination of dioxygen to the metal center.[6a,57]

Mulliken charge population analysis (Table 6) confirms that the degree of dioxygen reduction decreases in going from $LCuO_2$ to L^1CuO_2 to L^2CuO_2 in both the end-on and side-on cases. This in turn is fully consistent with the aforementioned decreases in O–O bond length and increases in ν(O–O) which occurs upon CF_3 substitution. These three trends combined indicate that while η^2-$LCuO_2$ lies far to the Cu(III)–peroxide side[7,10] of the Cu(II)–superoxide/Cu(III)–peroxide continuum,[9] the side-on oxygen complexes supported by L^1 and L^2 each possess more Cu(II)–superoxide than the former. The narrow range of these trends, however, indicates that the overall electronic differences between η^2-$LCuO_2$, η^2-L^1CuO_2, and η^2-L^2CuO_2 are relatively small and thus the inductive effect of the CF_3 groups, while unmistakable, is nonetheless minor.

Finally, the effects of CF_3 substitution on the reactivity of the Cu/O_2 adducts were assessed by theoretical evaluation of the capability of the adducts to abstract H atoms from hydrocarbons. This can be measured by determining the O–H bond dissociation energies (BDEs) for the O–H bonds formed upon hydrogen atom abstraction. With the side-on Cu/O_2 adducts, the BDEs rise from 54.9 kcal mol^{-1} to 58.7 kcal mol^{-1} in going from L to L^2 (Table 7). The O–H BDEs for the end-on adducts are relatively insensitive to changes in the ligand backbone at ∼60 kcal mol^{-1} (Table S6).‡ Comparison to C–H BDEs such as those for 1,4-cyclohexadiene (73.0 kcal mol^{-1})[58] and the benzylic position in the physiological substrate for DβM,[59] dopamine (87.2 kcal mol^{-1}),[11b] implies that the 1 : 1 adducts supported by each of L, L^1, and L^2 should be unreactive towards substrates. Despite the observed ∼4 kcal mol^{-1} increase in potency for the side-on adducts upon CF_3 substitution into the ligand backbone, their ability to attack substrate nonetheless remains well below that predicted for Cu(III)–oxo species.[11b,12d,e]

§ DFT calculations have systematically overestimated O–O stretching frequencies in 1 : 1 Cu/O_2 adducts.[7b,8,53] This is most likely attributable to the challenge of obtaining a sufficiently accurate wave function for these multideterminantal species within the framework of DFT (see computational methods).[34] While *quantitative* comparison to experimental ν(O–O) may therefore be problematic, *qualitative* comparisons to experimental ν(O–O) values and analysis of the *relative* computed ν(O–O) values provide useful insights into the nature of the Cu/O_2 species.

Table 7 Calculated reduction potentials and pK_b values for the singlet side-on Cu/O_2 adducts and gas phase bond dissociation energies (BDEs) for a hydrogen atom bound to the dioxygen fragment

Complex	E°[a]	pK_b[b]	BDE[c]
$LCuO_2$	−2.06[d]	14.1[d]	54.9
L^1CuO_2	−1.81	17.5	56.8
L^2CuO_2	−1.56	23.4	58.7

[a] Units: V *vs.* SHE, at −80 °C in THF. [b] At 25 °C in H_2O. [c] Units: kcal mol^{-1}. [d] Ref. 11*b*.

Decomposing hydrogen atom abstraction into its components[60]—transfer of a proton and transfer of an electron from substrate to the 1 : 1 adduct—provides insight into the origin of the lack of reactivity with the 1 : 1 Cu/O_2 species (for details, see ESI‡ text and Tables S2–S5).‡ Low reduction potentials and high pK_b values for the 1 : 1 Cu/O_2 adducts (Tables 7, S6)‡ indicate significant stability toward reduction or protonation.[11b] These same data reveal that, as the electron donating capability of the ligand is decreased by incrementing the number of CF_3 backbone groups, the reduction potentials and pK_b values both increase. The former trend in particular mirrors that seen in the experimental redox potentials for the Cu(I)–MeCN complexes, which also increased by 200–300 mV upon substitution of each CF_3 group (*cf.* Table 2). In sum, reduction becomes promoted while protonation is deterred, and these effects offset one another to lead to minimal change in the O–H BDEs, and hence reactivity, among the Cu/O_2 adducts supported by each of L, L^1, and L^2.

Conclusions

Copper(I)–acetonitrile complexes with the ligands L^1 and L^2, and the series (L, L^1 or L^2)Cu(CO) were prepared and characterized. Along with the previously reported complex $LCu(CH_3CN)$, these copper(I) species provided the means for an examination of the potential to electronically tune the β-diketiminate ligand and thereby influence the outcomes of Cu(I)/O_2 reactivity. As such, the donating ability of the ligands was assessed through comparisons of the redox potentials of the nitrile adducts and the carbonyl stretching frequencies of the carbon-monoxide adducts. The shift in potential for the Cu(I/II) redox pair in going from L to L^1 to L^2 (spanning ∼500 mV) reflects the electronic destabilisation of the Cu(II) state—a direct consequence of the lessened ligand electron donation upon CF_3 substitution. For $L^2Cu(CH_3CN)$, the redox potential alone is suggestive of a ligand environment not conducive to O_2 reactivity. The increase in ν(CO) with increasing ligand backbone fluorination is substantial and the trend correlates with the redox potential data.

While $L^1Cu(CH_3CN)$ undergoes rapid oxygenation with O_2, L^2 does not support the formation of a Cu/O_2 adduct. $L^1Cu(O_2)$ was formulated as a side-on bound Cu(III)–peroxo complex on the basis of electronic and vibrational spectroscopy, including similarities with $LCu(O_2)$, and theoretical predictions that coincided with the observed oxygen-isotope sensitivity of the O–O vibration. Although the presence of one CF_3 substituent (L^1) had a small effect on the Cu/O_2 chemistry relative to the case for L (as gauged by the slight shift in ν(O–O) for its 1 : 1 adduct), the electronics

are clearly perturbed in such a way that the presence of two CF_3 substituents (L^2) prevents formation of a Cu/O_2 intermediate. Further, the theoretical comparisons for oxygenation of (L, L^1 or L^2)$Cu(CH_3CN)$ indicate that the formation of an end-on 1 : 1 Cu/O_2 adduct requires a less-donating β-diketiminate ligand (such as L^2), though this in itself proves to be an experimental obstacle given that such ligands give rise to an endergonic oxygenation process. Thus, future efforts in developing a bidentate ligand that supports an end-on 1 : 1 Cu/O_2 adduct face the challenge of balancing suitable ligand electronics with experimentally feasible (thermodynamically favorable) oxygenation of the Cu(I) complex.

Acknowledgements

We thank the NIH (Grant GM47365 to W. B. T., Grant NRSA-GM070144 to B. F. G.) and the NSF (Grant CHE-0203346 to C. J. C.) for financial support. We also thank Dr Victor G. Young, Jr. for assistance with X-ray data collection and refinement, and Professor Lawrence Que, Jr. for the use of resonance Raman spectroscopy instrumentation. Elizabeth Devine and Nicole Settergren are thanked for initial experimental efforts. We are also grateful to the reviewers for their helpful suggestions.

References

1 (*a*) M. A. Halcrow, in *Comprehensive Coordination Chemistry II*, ed. J. A. McCleverty and T. J. Meyer, Elsevier: Amsterdam, 2004, vol. 8, pp. 395; (*b*) S. Itoh, *Curr. Opin. Chem. Biol.*, 2006, **10**, 115.
2 I. Arends, P. Gamez and R. A. Sheldon, *Adv. Inorg. Chem.*, 2006, **58**, 235.
3 (*a*) L. M. Mirica, X. Ottenwaelder and T. D. P. Stack, *Chem. Rev.*, 2004, **104**, 1013; (*b*) E. A. Lewis and W. B. Tolman, *Chem. Rev.*, 2004, **104**, 1047.
4 S. T. Prigge, B. A. Eipper, R. E. Mains and L. M. Amzel, *Science*, 2004, **304**, 864.
5 (*a*) K. Fujisawa, M. Tanaka, Y. Moro-oka and N. Kitajima, *J. Am. Chem. Soc.*, 1994, **116**, 12079; (*b*) P. Chen, D. E. Root, C. Campochiaro, K. Fujisawa and E. I. Solomon, *J. Am. Chem. Soc.*, 2003, **125**, 466.
6 (*a*) M. Schatz, V. Raab, S. P. Foxon, G. Brehm, S. Schneider, Markus Reiher, M. C. Holthausen, J. Sundermeyer and S. Schindler, *Angew. Chem., Int. Ed.*, 2004, **43**, 4360; (*b*) C. Würtele, E. Gaoutchenova, K. Harms, M. C. Holthausen, J. Sundermeyer and S. Schindler, *Angew. Chem., Int. Ed.*, 2006, **45**, 3867.
7 (*a*) N. W. Aboelella, E. A. Lewis, A. M. Reynolds, W. W. Brennessel, C. J. Cramer and W. B. Tolman, *J. Am. Chem. Soc.*, 2002, **124**, 10660; (*b*) N. W. Aboelella, S. V. Kryatov, B. F. Gherman, W. W. Brennessel, V. G. Young, Jr., R. Sarangi, E. V. Rybak-Akimova, K. O. Hodgson, B. Hedman, E. I. Solomon, C. J. Cramer and W. B. Tolman, *J. Am. Chem. Soc.*, 2004, **126**, 16896.
8 A. M. Reynolds, B. F. Gherman, C. J. Cramer and W. B. Tolman, *Inorg. Chem.*, 2005, **44**, 6989.
9 C. J. Cramer, W. B. Tolman, K. H. Theopold and A. L. Rheingold, *Proc. Natl. Acad. Sci. USA*, 2003, **100**, 3635.
10 R. Sarangi, N. Aboelella, K. Fujisawa, W. B. Tolman, B. Hedman, K. O. Hodgson and E. I. Solomon, *J. Am. Chem. Soc.*, 2006, **128**, 8286.
11 (*a*) A. M. Reynolds, E. L. Lewis, N. W. Aboelella and W. B. Tolman, *Chem. Commun.*, 2005, 2014; (*b*) B. F. Gherman, W. B. Tolman and C. J. Cramer, *J. Comput. Chem.*, 2006, in press.
12 (*a*) J. P. Evans, K. Ahn and J. P. Klinman, *J. Biol. Chem.*, 2003, **278**, 49691; (*b*) P. Chen and E. I. Solomon, *J. Am. Chem. Soc.*, 2004, **126**, 4991; (*c*) B. F. Gherman, D. E. Heppner, W. B. Tolman and C. J. Cramer, *J. Biol. Inorg. Chem.*, 2006, **11**, 197; (*d*) T. Kamachi, N. Kihara, Y. Shiota and K. Yoshizawa, *Inorg. Chem.*, 2005, **44**, 4226; (*e*) K. Yoshizawa, N. Kihara, T. Kamachi and Y. Shiota, *Inorg. Chem.*, 2006, **45**, 3034.
13 (*a*) C. X. Zhang, S. Kaderli, M. Costas, E. Kim, Y.-M. Neuhold, K. D. Karlin and A. D. Zuberbühler, *Inorg. Chem.*, 2003, **42**, 1807; (*b*) J. Shearer, C. X. Zhang, L. N. Zakharov, A. L. Rheingold and K. D. Karlin, *J. Am. Chem. Soc.*, 2005, **127**, 5469.
14 M. J. Henson, M. A. Vance, C. X. Zhang, H.-C. Liang, K. D. Karlin and E. I. Solomon, *J. Am. Chem. Soc.*, 2003, **125**, 5186.
15 A. J. Johansson, M. R. A. Blomberg and P. E. M. Siegbahn, *Inorg. Chem.*, 2006, **45**, 1491.
16 T. Osako, S. Terada, T. Tosha, S. Nagatomo, H. Furutachi, S. Fujinami, T. Kitagawa, M. Suzukib and S. Itoh, *Dalton Trans.*, 2005, 3514.
17 H. V. R. Dias and T. K. H. H. Goh, *Polyhedron*, 2004, **23**, 273, and references cited therein.
18 (*a*) Z. Hu, R. D. Williams, D. Tran, T. G. Spiro and S. M. Gorun, *J. Am. Chem. Soc.*, 2000, **122**, 3556; (*b*) Z. Hu, G. N. George and S. M. Gorun, *Inorg. Chem.*, 2001, **40**, 4812.
19 G. Aullón, S. M. Gorun and S. Alvarez, *Inorg. Chem.*, 2006, **45**, 3594.
20 D. S. Laitar, C. J. N. Mathison, W. M. Davis and J. P. Sadighi, *Inorg. Chem.*, 2003, **42**, 7354.
21 H. V. R. Dias and S. Singh, *Inorg. Chem.*, 2004, **43**, 5786.
22 J. A. J. Jarvis, R. Pearce and M. F. Lappert, *J. Chem. Soc., Dalton Trans.*, 1977, 999.
23 D. T. Carey, E. K. Cope-Eatough, E. Vilaplana-Mafé, F. S. Mair, R. G. Pritchard, J. E. Warren and R. J. Woods, *Dalton Trans.*, 2003, 1083.
24 D. J. E. Spencer, N. W. Aboelella, A. M. Reynolds, P. L. Holland and W. B. Tolman, *J. Am. Chem. Soc.*, 2002, **124**, 2108.
25 N. G. Connelly and W. E. Geiger, *Chem. Rev.*, 1996, **96**, 877.
26 *SMART v5.054*, Bruker Analytical X-Ray Systems, Madison, WI, 2001.
27 An empirical correction for absorption anisotropy: R. Blessing, *Acta Crystallogr., Sect. A.*, 1995, **A51**, 33.
28 For $L^2Cu(CH_3CN)$: *SAINT v6.2*, Bruker Analytical X-Ray Systems, Madison, WI, 2001; For $L^1Cu(CH_3CN)$, LCu(CO) and $L^2Cu(CO)$: *SAINT+ v6.45*, Bruker Analytical X-Ray Systems, Madison, WI, 2003.
29 *Jaguar 6.1. Schrodinger*, LLC: Portland, Oregon, 2003.
30 B. G. Johnson, P. M. W. Gill and J. A. Pople, *J. Chem. Phys.*, 1993, **98**, 5612.
31 A. D. Becke, *J. Chem. Phys.*, 1993, **98**, 1372.
32 C. T. Lee, W. T. Yang and R. G. Parr, *Phys. Rev. B*, 1988, **37**, 785.
33 J.-M. Ducere, A. Goursot and D. Berthomieu, *J. Phys. Chem. A*, 2005, **109**, 400.
34 B. F. Gherman and C. J. Cramer, *Inorg. Chem.*, 2004, **43**, 7281.
35 N. W. Aboelella, B. F. Gherman, L. M. R. Hill, J. T. York, N. Holm, V. G. Young, Jr., C. J. Cramer and W. B. Tolman, *J. Am. Chem. Soc.*, 2006, **128**, 3345.
36 (*a*) P. J. Hay and W. R. Wadt, *J. Chem. Phys.*, 1985, **82**, 270; (*b*) W. R. Wadt and P. J. Hay, *J. Chem. Phys.*, 1985, **82**, 284; (*c*) P. J. Hay and W. R. Wadt, *J. Chem. Phys.*, 1985, **82**, 299.
37 R. A. Friesner, M.-H. Baik, V. Guallar, B. F. Gherman, M. Wirstam, R. B. Murphy and S. J. Lippard, *Coord. Chem. Rev.*, 2003, **238–239**, 267.
38 M.-H. Baik, M. Newcomb, R. A. Friesner and S. J. Lippard, *Chem. Rev.*, 2003, **103**, 2385.
39 C. W. Bauschlicher and H. Partridge, *J. Chem. Phys.*, 1995, **103**, 1788.
40 B. Marten, K. Kim, C. Cortis, R. A. Friesner, R. B. Murphy, M. N. Ringnalda, D. Sitkoff and B. Honig, *J. Phys. Chem.*, 1996, **100**, 11775.
41 D. J. Tannor, B. Marten, R. B. Murphy, R. A. Friesner, D. Sitkoff, A. Nicholls, M. N. Ringnalda, W. A. Goddard, III and B. Honig, *J. Am. Chem. Soc.*, 1994, **116**, 11875.
42 C. Carvajal, K. J. Tolle, J. Smid and M. Szwarc, *J. Am. Chem. Soc.*, 1965, **87**, 5548.
43 D. J. Metz and A. Glines, *J. Phys. Chem.*, 1967, **71**, 1158.
44 M. D. Tissandier, K. A. Cowen, W. Y. Feng, E. Gundlach, M. H. Cohen, A. D. Earhart, J. V. Coe and T. R. Tuttle, *J. Phys. Chem. A*, 1998, **102**, 7787.
45 C. P. Kelly, C. J. Cramer and D. G. Truhlar, *J. Phys. Chem. B*, 2006, **110**, 16066.
46 X. Ribas, D. A. Jackson, B. Donnadieu, J. Mahia, T. Parella, R. Xifra, B. Hedman, K. O. Hodgson, A. Llobet and T. D. P. Stack, *Angew. Chem., Int. Ed.*, 2002, **41**, 2991.
47 P. Winget, C. J. Cramer and D. G. Truhlar, *Theor. Chem. Acc.*, 2004, **112**, 217.
48 K. Pierloot, B. Dumez, P. O. Widmark and B. O. Roos, *Theor. Chim. Acta*, 1995, **90**, 87.

49 K. Andersson, P. A. Malmqvist and B. O. Roos, *J. Chem. Phys.*, 1992, **96**, 1218.
50 G. Karlstrom, R. Lindh, P. A. Malmqvist, B. O. Roos, U. Ryde, V. Veryazov, P. O. Widmark, M. Cossi, B. Schimmelpfennig, P. Neograd y and L. Seijo, *Comput. Mater. Sci.*, 2003, **28**, 222.
51 Z. Barandiaran and L. Seijo, *Can. J. Chem.*, 1992, **70**, 409.
52 B. F. Gherman, D. E. Heppner, W. B. Tolman and C. J. Cramer, *J. Biol. Inorg. Chem.*, 2006, **11**, 197.
53 N. W. Aboelella, B. F. Gherman, L. M. R. Hill, J. T. York, N. Holm, V. G. Young, Jr., C. J. Cramer and W. B. Tolman, *J. Am. Chem. Soc.*, 2006, **128**, 3445.
54 A value of $E_{1/2} = -215$ mV *vs.* Fc/Fc^{+} was reported previously for $LCu(CH_3CN)$ in CH_3CN: D. J. E. Spencer, A. M. Reynolds, P. L. Holland, B. A. Jazdzewski, C. Duboc-Toia, L. L. Pape, S. Yokota, Y. Tachi, S. Itoh and W. B. Tolman, *Inorg. Chem.*, 2002, **41**, 6307.
55 D. B. Rorabacher, *Chem. Rev.*, 2004, **104**, 651.
56 D. W. Randall, S. DeBeer, P. L. Holland, B. Hedman, K. O. Hodgson, W. B. Tolman and E. I. Solomon, *J. Am. Chem. Soc.*, 2000, **122**, 11632.
57 C. R. Kinsinger, B. F. Gherman, L. Gagliardi and C. J. Cramer, *J. Biol. Inorg. Chem.*, 2005, **10**, 778.
58 D. R. Lide, *Handbook of Chemistry and Physics, 85th Edition*, CRC Press, Boca Raton, 2004.
59 (*a*) J. P. Klinman, *Chem. Rev.*, 1996, **96**, 2541; (*b*) L. C. Stewart and J. P. Klinman, *Annu. Rev. Biochem.*, 1988, **57**, 551.
60 J. M. Mayer, *Acc. Chem. Res.*, 1998, **31**, 441.